Desalination 404 (2017) 192–199

Contents lists available at ScienceDirect

Desalination

journal homepage: www.elsevier.com/locate/desal

Experimental investigation of adsorption water desalination/cooling system using CPO-27Ni MOF

Peter G. Youssef *, Hassan Dakkama, Saad M. Mahmoud, Raya K. AL-Dadah

School of Mechanical Engineering, University of Birmingham, Birmingham B15 2TT, UK

HIGHLIGHTS

- Experimental - numerical study of CPO-27Ni MOF for adsorption desalination/cooling
- Effects of Condenser and evaporator water inlet temperatures are studied.
- Simulink model is developed, validated and used to study other operating conditions.
- CPO-27Ni produced water and cooing of 23m^3/day & 216 Rton per ton·ads, respectively.

ARTICLE INFO

Article history:
Received 18 August 2016
Received in revised form 7 September 2016
Accepted 5 November 2016
Available online 18 November 2016

Keywords:
Experimental
Adsorption
CPO-27(Ni)
Desalination
Cooling
Seawater

ABSTRACT

Although many adsorbent materials have been used in adsorption systems, only silica-gel was tested experimentally for desalination applications. This work experimentally and numerically investigates the use of CPO-27(Ni) an advanced Metal Organic Framework-MOF adsorbent material in a 1-bed adsorption system for water desalination and cooling applications. Operating parameters as switching time, half cycle time, evaporator and condenser water inlet temperatures were studied to investigate their effects on cycle water production and cooling. Moreover, a mathematical simulation model is developed, validated and used to predict cycle outputs at other operating conditions. Results showed that as evaporator temperature increases and condenser temperature decreases, cycle outputs increase. Also, it was shown that adsorption desalination cycles can work with condenser pressure lower than evaporator pressure as the cycle is an open loop one (i.e. no refrigerant is flowing back from condenser to evaporator). A water production of 22.8 m^3/tonne·ads/day was achieved using 40 °C evaporator temperature, 5 °C condenser temperature and 95 °C desorption temperature. Similar water production can be achieved using 30 °C condensing temperature but at 120 °C desorption temperature. For space cooling applications (T_{evap} < 20 °C), cycle cooling produced was found to be 65 Rton/tonne·ads. This work highlights the potential of using advanced MOF materials for water desalination/ cooling applications.

1. Introduction

Many countries depend on water desalination technologies to meet their potable water needs. Four water desalinating techniques are widely used which are reverse osmosis (RO), multistage flash (MSF), multi-effect distillation (MED) and mechanical vapor compression (MVC) [1]. However, these techniques suffer from high power consumption which in turn increases CO_2 emissions and water production costs [2,3]. Recently adsorption desalination technology was reported to outperform the current conventional technologies in terms of high grade fresh potable water of salinity as low as 10 ppm, lower electric energy consumption of 1.38 kWh/m^3 and CO_2 emission of 0.6 kg/m^3 while having lower water production cost of 0.2$/m^3 [4].

The adsorption water desalination cycle consists of three main components namely adsorption/desorption bed, evaporator and condenser producing desalinated water (from condenser) and cooling (from evaporator) [5–9]. The desalination/refrigeration adsorption system depends on the combination of four processes; evaporation due to adsorption and condensation as a result of desorption. Seawater is fed into the evaporator where it is evaporated as a result of the associated adsorption process while extracting heat from the chilled water passing through the evaporator coil producing the cooling effect in this cycle [6, 10]. In the adsorption process, water vapor is adsorbed by the adsorbent material while in the desorption process the water vapor is regenerated by heating and the desorbed water vapor is then condensed in the condenser producing fresh water [11,12].

Different adsorbent materials including silica-gel and zeolite have been reported for desalination applications using different cycle configurations. Thu et al. [13] experimentally tested an adsorption

* Corresponding author.
E-mail address: petergeorge@live.com (P.G. Youssef).

http://dx.doi.org/10.1016/j.desal.2016.11.008
0011-9164/

Nomenclature

c_p	specific heat at constant pressure (kJ·kg^{-1}·K^{-1})
h	enthalpy (kJ·kg^{-1})
M	mass (kg)
$\dot{m}$	mass flow rate (kg·s^{-1})
n	adsorption/Desorption phase, flag (−)
P	pressure (kPa)
Q_{st}	isosteric heat of adsorption (kJ/kg)
SCP	specific cooling power (Rton·t^{-1})
SDWP	specific daily water production (m^3·t^{-1}·day^{-1})
T	temperature (K)
W	uptake (kg·kg^{-1})
W^*	equilibrium uptake (kg·kg^{-1})
X	salt concentration (ppm)
θ	seawater charging flag (−)
γ	brine discharge flag (−)
τ	no. of cycles per day (−)

Subscripts

a	adsorbent material
ads	adsorption
b	brine
cond	condenser
cw	cooling water
D	vapor
d	distillate water
des	desorption
evap	evaporator
f	liquid
hw	heating water
HX	heat exchanger
in	inlet
ads	adsorber bed
des	desorber bed
out	outlet
s	seawater
t	time

desalination system operates in two and four bed modes. Heating source temperature and cycle time have been examined during their tests for the two operating modes. It was found that as heat source temperature decreases, longer cycle time is required to obtain the highest water production. In addition, in two bed mode, maximum water production reported was 8.7 m^3/tonne of silica-gel/day when 85 °C hot source temperature was used while for four bed mode, at the same heating temperature, 10 m^3/tonne of silica-gel/day was produced.

Ng et al. [8], have used a 215 m^2 solar collector to obtain the required heating for regeneration of water vapor in a 2 bed silica-gel adsorption system for water desalination and cooling applications. The solar collector produced heat source temperature varying from 65 to 80 °C which used to produce 3–5 m^3 of desalinated water and cooling in the range of 25–35 Rton/tonne of silica-gel at chilled water temperature of 7 to 10 °C.

Mitra et al. [14], have introduced a new adsorption cycle for desalination and cooling. This system has 2 stages with 2 beds per stage. Simulations as well as experiments have been carried out at different evaporator pressures and half cycle times to predict desalinated water output, cooling capacity and coefficient of performance (COP). Results showed that maximum produced desalinated water is 1 m^3/tonne silica-gel/day while cooling capacity is 7.5 Rton/tonne silica-gel with COP value of 0.25. These results were obtained at evaporator pressure of 1.7 kPa and half cycle time of 1800 s. The authors attributed these low production capacities, compared to literature, to the quite high ambient temperature, 41 °C, which affected the performance of the air cooled condenser. In addition, 2–3 times larger silica gel particle sizes than those reported in literature were used which resulted in slower adsorption/desorption rates.

Youssef et al. [15], have studied the use of advanced zeolite material, AQSOA-Z02, for adsorption desalination and cooling applications. In their work, a comparison between the AQSOA-ZO2 and silica-gel has been performed when operating in a two bed adsorption cycle for the production of desalinated water and cooling. The key parameters of the comparison are SDWP and specific cooling power (SCP) while different heating source temperatures and evaporator water inlet temperatures were applied. It was found that AQSOA-Z02 is less sensitive than silica gel to evaporator water temperature variations. Accordingly, AQSOA-Z02 outperformed silica-gel at lower evaporator water temperatures <25 °C where at 10 °C evaporator water temperature, AQSOA-Z02 cycle can produce 5.8 m^3 water per day and 50.1 Rton of cooling while silica-gel cycle generate only SDWP of 2.8 m^3 and SCP of 17.2 Rton. On the other hand, at the same heating temperature of 85 °C but at 30 °C evaporator water temperature silica-gel cycle produces maximum SDWP of 8.4 m^3 and 62.4 Rton of cooling.

Youssef et al. [16], have investigated the use of AQSOA-Z02 in a novel adsorption system consisting of evaporator, condenser, integrated evaporator-condenser device and 4 adsorber beds. Results showed that by utilizing heat recovery between system components, water production can reach 12.4 m^3/tonne adsorbent/day and cooling of 32.4 Rton/tonne adsorbent at evaporator inlet water temperature of 10 °C. Also, results showed that this system can produce 15.4 m^3/tonne adsorbent/day of desalinated water if no cooling is required.

Ali et al. [17], have presented a double stage system to produce cooling through stage-1 and desalinated water from condensers of stages 1 and 2. AQSOA-Z02 and silica-gel were used as adsorbents in the two stages, 1 and 2 respectively. A heat recovery was implemented between condensers and evaporators of the system to reduce condenser pressure and increase evaporator pressure which resulted in increased cycle outputs. Results showed that this new configuration produced more water by 26% and 45% more cooling compared to the conventional adsorption desalination and cooling systems.

Elsayed et al. [18] have investigated numerically the potential of using two metal organic framework adsorbent materials (MOF) for different adsorption applications including water desalination and cooling. Isotherms, kinetics and cycle stability were measured for both CPO-27(Ni) and Aluminum fumarate MOF materials where the maximum uptake was 0.47 and 0.53 $kg_{water}/kg_{adsorbent}$ respectively. It was found that at high desorption temperatures (>90 °C) and low evaporation temperature (5 °C), CPO-27(Ni) outperforms Al-Fumarate. However, Al-Fumarate resulted in better performance at high evaporation temperature of 20 °C and/or low bed heating temperature of 70 °C.

All reviewed work on water adsorption desalination, showed that silica-gel/water is the only working pairs investigated experimentally. This work, experimentally investigates the use of an advanced metal organic frameworks adsorbent material, (CPO-27Ni, produced by Johnson Matthey Ltd.) in a 1 bed adsorption cycle for production of fresh water and cooling. In addition, a numerical simulation is carried out, validated and used to predict the system performance at other operating conditions.

2. Experimental test facility

Fig. 1 shows a schematic diagram for a lab scale adsorption test facility developed for the production of fresh water and cooling using CPO-27Ni MOF material as an adsorbent. The main components of this system are: adsorption bed, evaporator and condenser shown pictorially in Fig. 2.

In such adsorption water desalination system, seawater is supplied to the evaporator where it evaporates during the adsorption half cycle while the adsorber bed is connected to the evaporator. During

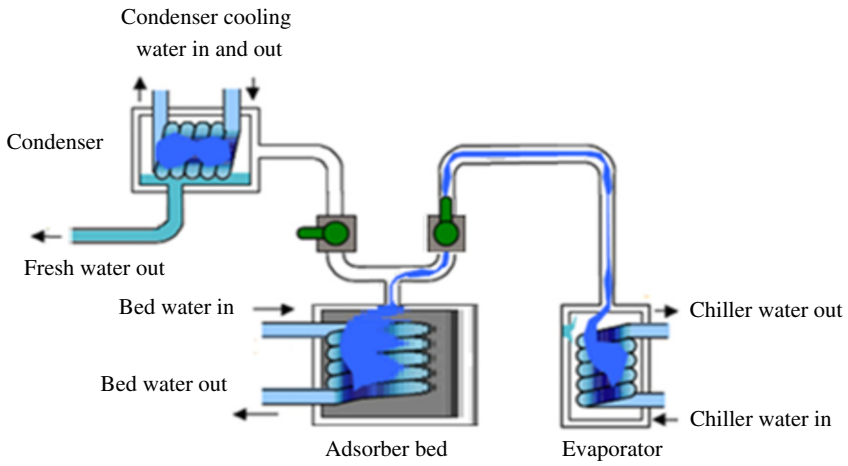

Fig. 1. Schematic diagram for a 1-bed adsorption.

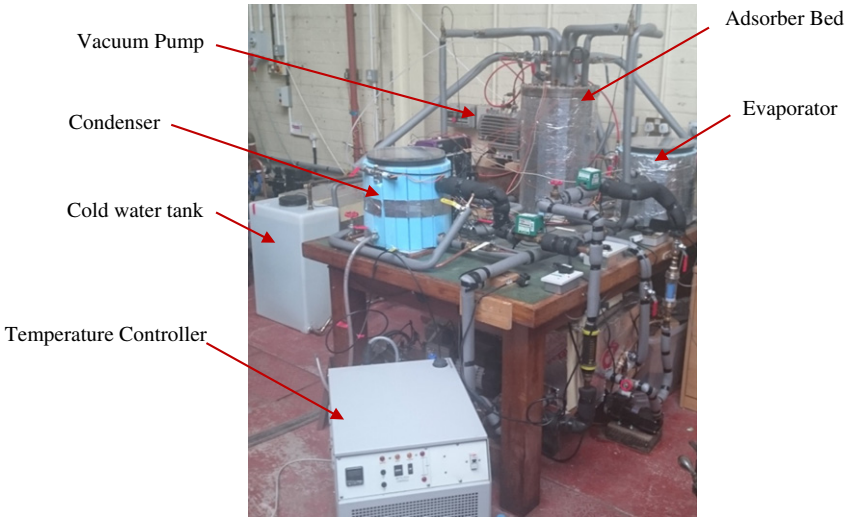

Fig. 2. Pictorial view for the single-bed adsorption test rig.

adsorption time, cooling water is circulated in the adsorption bed to absorb the released heat from the adsorbent material. Then, in the desorption phase, the bed is heated by hot water and water vapor is regenerated. During this desorption process, the adsorber bed is connected to the condenser where the water vapor is condensed producing fresh water. As shown in Fig. 2, there are other auxiliary components in the system which are heating and cooling water systems for the bed and temperature controllers to supply constant water temperatures for the evaporator and condenser. In addition, there are vacuum pumps to generate the required vacuum pressure in the system. Adsorber bed as shown in Fig. 3 is a rectangular finned tube heat exchanger with the adsorbent material packed between the fins and surrounded by a metal mesh to keep adsorbent particles in position. The evaporator and condenser are cylindrical vacuum designed chambers with helically shaped cooling coil.

The experimental test facility is equipped with TJC100-CPSS T-type thermocouples to measure the temperature of the evaporator liquid and gas, adsorbent material in bed and vapor in the bed space. In the condenser, RS-pro, K-type thermocouples are used for measuring vapor and condensed water temperatures. Platinum RTD temperature sensors were used to measure bed heating and cooling water inlet and outlet temperatures, evaporator and condenser circulating water inlet and outlet temperatures. The evaporator, condenser and adsorber bed pressures are measured using pressure transducers with an accuracy of ±0.01 kPa. Flowmeters of type FLC-H14 (0–57 LPM) are used to measure the adsorber bed heating/cooling water flowrate manually with an accuracy of ±1 L while flowrates of condenser and evaporator water circuits are measured by Parker type flowmeter (2–30 LPM) with an accuracy of ±5%. Details of the system component specifications are presented in Table 1.

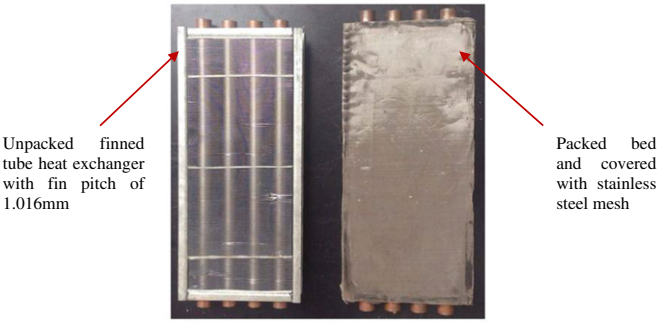

Fig. 3. Pictorial view for the adsorber bed.

Table 1
System specifications.

Property	Value
System specifications	
Adsorbent mass	0.67 kg
Bed metal mass	29.3 kg
Evaporator metal mass	15.1 kg
Condenser metal mass	15.1 kg
Bed heat transfer area	2.55 m^2
Evaporator heat transfer area	0.11 m^2
Condenser heat transfer area	0.16 m^2

Table 2
Physical Properties of CPO-27Ni.

Property	Value
Pore mean diameter	0.7 nm
Surface area	299 m^2/g
Total Pore volume	217 cm^3/kg

Table 3
Dubinin-Astakhov equation constants.

Symbol	Value	Unit[a]
W^∞	0.46826	kg/kg of adsorbent
E	10.0887	kJ/mol
n	5.6476	(−)
R	8314	J/mol·K

[a] Units are; kg = kilogram, K = Kelvin.

Table 4
Linear driving force, LDF equation constants.

Symbol	Pr < 0.2	Pr > 0.2	Unit
k_o	81.5615	0.7779	1/s
E_a	3.2006E4	1.4806E4	J/mol

Pr is the pressure ratio between bed and heat exchanger.
Units are; s = second, J = Joule, mol = mole.

3. Adsorbent material characteristics

CPO-27Ni used in this work is an MOF adsorbent manufactured commercially by Johnson Matthey. Fig. 4 shows SEM image for this adsorbent material and its physical properties are listed in Table 2 [19–21].

For prediction of adsorbent material performance, two parameters are required namely adsorption isotherms and kinetics. The maximum amount of adsorbate that can be adsorbed per unit mass of dry material at a certain pressure ratio is called 'adsorption isotherms' while the rate of adsorption or desorption at the operating pressure ratio is called 'adsorption kinetics'. The pressure ratio is defined as the ratio between evaporator to bed pressures during adsorption process or ratio between condenser to bed pressure during desorption process. CPO-27Ni isotherms are modelled using Dubinin-Astakhov (D-A) model (Eqs. 1 & 2) [22] with the constants given in Table 3 [23].

$$W^* = W^\infty \exp\left[-\left(\frac{A}{E}\right)^n\right] \tag{1}$$

where W^* is the predicted equilibrium uptake, W^∞ is the adsorbed water vapor mass based on the total accessible pore volume [kg_{ref}/kg_{ads}], E is the characteristic energy [J/mol], n is an empirical constant and A, is the adsorption potential which is given by:

$$A = -RTln\left(\frac{P}{P_o}\right) \tag{2}$$

$$\frac{dW}{dt} = k(W^* - W) \tag{3}$$

$$k = k_o\, e^{\left(\frac{-Ea}{RT}\right)} \tag{4}$$

where R is the universal gas constant, T is the temperature of the adsorbent material and $\frac{P}{P_o}$ is the partial pressure ratio.

To determine adsorption kinetics, linear driving force (LDF) model commonly used to predict the rate of adsorption/desorption (Eqs. 3–4) [24]. Tests using dynamic vapor sorption (DVS) machine have been carried out at university of Birmingham, UK to determine the relation between uptake and time. By fitting the test results, the obtained constants of the LDF model are presented in Table 4 [23].

For assessment of adsorption desalination/cooling cycle performance, two parameters are calculated which are Specific Daily Water Production (SDWP) and Specific Cooling Power (SCP). SDWP is the amount of water produced per tonne of adsorbent per day while SCP is the amount of produced cooling per unit mass of adsorbent material used. These parameters are calculated using Eqs. 5–8 [6]:

$$SDWP = \int_0^{t_{cycle}} \frac{Q_{cond} \cdot \tau}{h_{fg} M_a} dt \tag{5}$$

$$SCP = \int_0^{t_{cycle}} \frac{Q_{evap} \cdot \tau}{M_a} dt \tag{6}$$

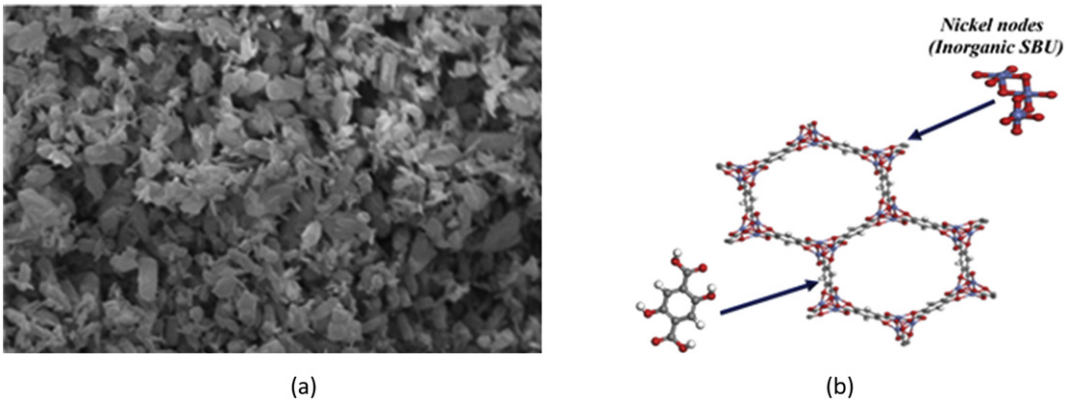

Fig. 4. SEM image (a) and crystal structure (b) for CPO-27Ni.

where:

$$Q_{cond} = \dot{m}_{cond} c_p (T_{cond}) (T_{cond,out} - T_{cond,in}) \quad (7)$$

$$Q_{evap} = \dot{m}_{chilled} c_p (T_{evap}) (T_{chilled,in} - T_{chilled,out}) \quad (8)$$

4. Results and discussion

As discussed in Section 3, adsorbent material performance depends on the partial pressure ratio determined by the adsorber bed and heat exchanger temperatures. For the material to work at low partial pressure ratio during desorption time ($P(T_{cond})/P(T_{des})$), this can be achieved either by increasing the heating fluid temperature or decreasing the condenser cooling water temperature. The operating temperature conditions used in this paper were selected to achieve partial pressure ratios ranging from 0.01 to 0.05 corresponding to condensing temperature ranging from 5 °C to 30 °C at fixed desorption temperature of 95 °C while adsorber bed cooling water is supplied from the mains at average temperature of 15 °C. Flowrates of water circuits in evaporator, condenser and adsorber beds are 4, 5 and 7.25 L/min respectively. Also, this work investigates the effect of other parameters like switching time, cycle time, evaporator water temperature and condenser water temperature on water production and cooling capacity.

4.1. Switching time effect

Switching time is the period of time when adsorbent bed is not connected neither to the evaporator nor to the condenser. During this time, adsorbent bed is either in precooling or in preheating process to be prepared for adsorption or desorption processes respectively. In this test, five switching times are tested from 5 to 1 min. at constant half cycle time of 14 min. Heating and cooling water temperatures are 95 °C and 16 °C while evaporator and condenser water temperatures are 10 °C. Fig. 5, shows the adsorber bed temperature through 5 consecutive cycles with switching time decreasing by 1 min every cycle. It can be seen that as switching time decreases, bed temperature profile becomes more smooth (as indicated by the two circles) leading to reducing the energy demand for heating and cooling the bed. Therefore the one-minute switching time was selected to be the best switching time for all further investigations.

4.2. Half cycle time effect

Half cycle time is the time for adsorption or desorption processes during the cycle when the bed is either connected to the evaporator or to the condenser. In this test six half cycle times were investigated ranging from 8 to18 min and their results are shown in Figs. 6 & 7.

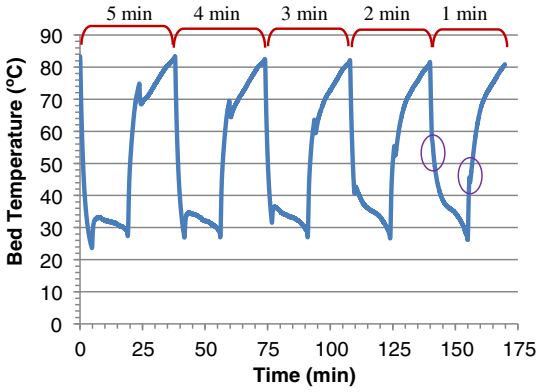

Fig. 5. Adsorbent bed temperature through 5 cycles at different switching times.

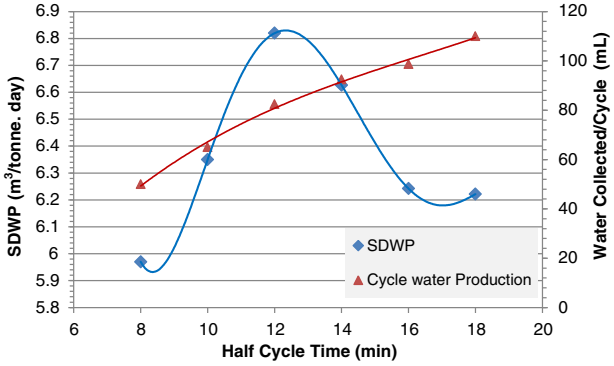

Fig. 6. SDWP and amount of collected water per cycle at different half cycle times.

Fig. 6 shows that as the half cycle time increases, the amount of water collected per cycle is increasing. However, by increasing cycle duration, number of cycles per day will decrease which adversely affects the daily water production. Results showed that half cycle time of 12 min can produce the maximum amount of daily water production of 6.8 m^3/tonne·ads/day. Regarding cooling output, Fig. 7 shows that as cycle time increases SCP decreases. This could be attributed to the evaporator temperature profile as it decreases at a higher rate at the beginning than at the end of the adsorption time which results in lower average evaporator temperature at shorter cycle times which in turn increases SCP. Although half cycle time of 10 min gives the highest SCP of 200 W/kg (57 Rton/tonne·ads), a time of 12 min is used for the rest of the experimental work since it results in maximum SDWP which is the main focus of this research.

4.3. Evaporator and condenser water temperature effect

Water desalination adsorption cycle is an open loop system which is characterized by seawater feed in the evaporator and desalinated fresh water extraction from the condenser. Accordingly, this cycle is unlike closed loop adsorption refrigeration systems which necessitate condenser pressure to be higher than evaporator pressure to allow flowing of the refrigerant from condenser to evaporator [25]. Different evaporator and condenser water inlet temperatures are investigated with the range of 10–40 °C and 5–30 °C, respectively. As shown in Figs. 8 and 9, increasing evaporator water temperature increases daily water production and specific cooling power. In contrast, decreasing condenser temperature increases cycle outputs due to the decrease in the operating partial pressure ratio thus allowing desorption process to reach low uptakes. By changing evaporator water inlet temperature from 10 to 40 °C, water production increases by 202% from 6.8 to 20.6 m^3/tonne·ads/day when operating at 10 °C condenser. On the other hand, decreasing condenser water inlet temperature from 30 to 5 °C, increases cycle water outputs by 135% from 3.2 to 7.5 m^3/tonne·ads/day at evaporator temperature of 10 °C.

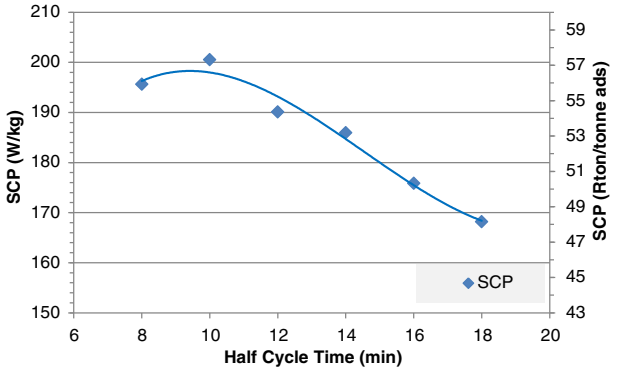

Fig. 7. SCP at different half cycle times.

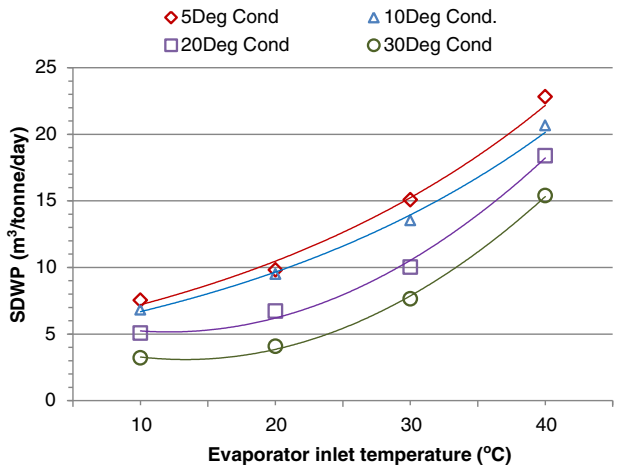

Fig. 8. SDWP at different evaporator and condenser water temperatures.

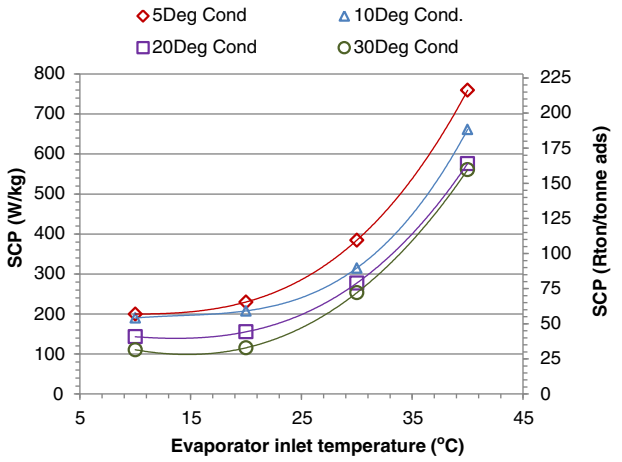

Fig. 9. SCP at different evaporator and condenser water temperatures.

Produced chilled water from the adsorption system can be used for cooling applications like space, process or district cooling [6]. Fig. 9 shows that this system can produce SCP of 225 W/kg for evaporator inlet temperature ranging from 10 °C to 20 °C suitable for space cooling. Also Fig. 9 shows that at evaporator inlet temperature ranging from 30 to 40 °C, SCP values can reach 750 W/kg which suitable for process cooling.

Fig. 10 shows temperature profiles of the main system components at two condenser temperatures of 5 and 30 °C while evaporator water inlet temperature is constant at 10 °C. Two line groups appear in these figures; the first is denoted by (L) and the other is denoted by (H) which refer to temperature profiles in case of low condenser temperature of 5 °C and high condenser temperature of 30 °C respectively.

As seen in Fig. 10-a, at lower condenser water inlet temperature of 5 °C with higher water production rates (i.e. higher uptake rate), bed temperature (point 1) cannot reach the low temperature of 22.8 °C (point 2) at the end of adsorption process and the high temperature of 84.9 °C (point 4) like the case of higher condenser temperature. This is due to the larger amount of heat released and extracted during adsorption and desorption processes respectively by the adsorbent material. In Fig. 10-b the hatched area represents the increase in cooling effect produced in the evaporator due to decreasing the condenser water inlet temperature which resulted in low evaporator temperature of 8 °C. In contrast, condenser temperature increases in case of 5 °C more than in case of 30 °C resulting in area 'B' larger than area 'A', Fig. 10-c, which is because of larger amount of water produced at lower condenser water inlet temperature.

5. Numerical simulation and validation

A Simulink model has been developed to simulate the adsorption water desalination/cooling system shown in Fig. 1. This model has been validated using the experimental results and then used to predict the system performance at other operating conditions.

5.1. Numerical model

In order to study the cycle, energy equations are solved for evaporator, condenser, adsorber/desorber bed in addition to mass and salt balance equations for the evaporator [26] as shown in Eqs. 9–13:

Evaporator mass balance equation:

$$\frac{dM_{s,evap}}{dt} = \theta \dot{m}_{s,in} - \gamma \dot{m}_b - n \cdot \frac{dW_{ads}}{dt} M_a \tag{9}$$

Evaporator salt balance equation:

$$M_{s,evap} \frac{dX_{s,evap}}{dt} = \theta X_{s,in} \dot{m}_{s,in} - \gamma X_{s,evap} \dot{m}_{brine} - n \cdot X_D \frac{dW_{ads}}{dt} M_a \tag{10}$$

Evaporator energy balance equation:

$$\begin{aligned}\left[M_{s,evap} c_{p,s}\right)(T_{evap}, X_{s,evap}) + M_{HX,Evap} c_{p,HX}\right] \frac{dT_{evap}}{dt} \\ = \theta \cdot h_f(T_{evap}, X_{s,evap}) \dot{m}_{s,in} - n \cdot h_{fg}(T_{evap}) \frac{(dW_{ads})}{dt} M_a \\ + \dot{m}_{chilled} c_p(T_{evap}) \\ \times (T_{(chilled\ in)} - T_{(chilled\ out)}) - \gamma h_f(T_{evap}, X_{s,evap}) \dot{m}_b\end{aligned} \tag{11}$$

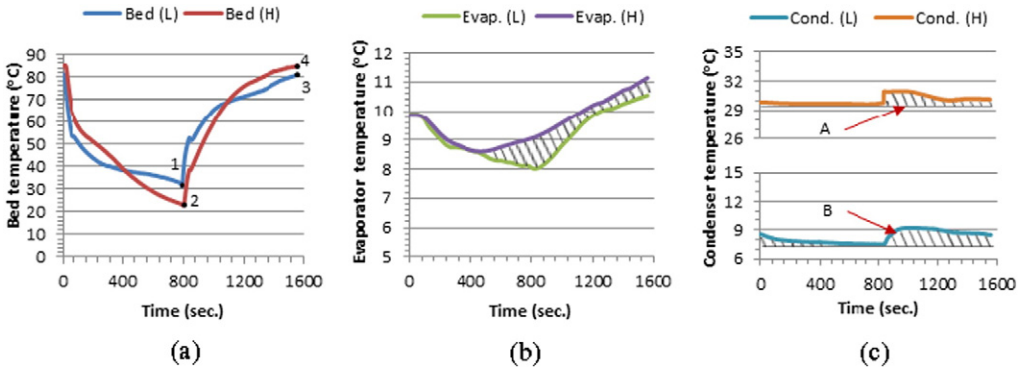

Fig. 10. Temperature profile at two condenser water inlet temperatures, 5 °C (L) and 30 °C (H) (a) Adsorber Bed (b) Evaporator (c) Condenser.

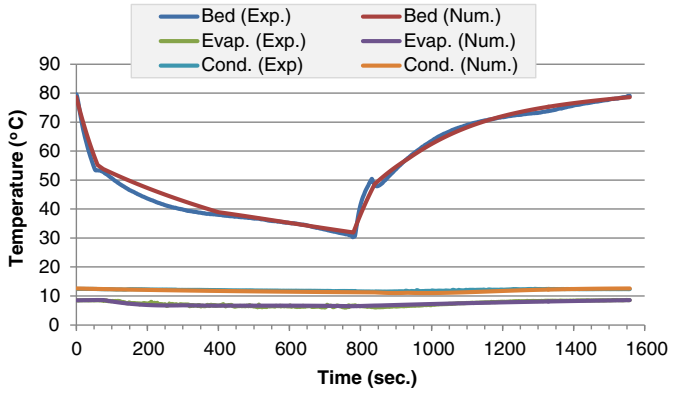

Fig. 11. Comparison of basic cycle components temperatures for numerical and experimental results of a single-bed adsorption desalination cycle.

Adsorption/desorption bed, energy balance equation:

$$\left[M_a c_{(p,a)} + M_{HX} c_{(p,HX)} + M_{abe} c_{p,abe}\right] \frac{dT_{ads/des}}{dt} = \pm m_{(cw/hw)} c_p \left(T''_{cw/hw,in} - T_{cw/hw,out}\right) \pm z \cdot Q_{st} M_a \frac{dW_{ads/des}}{dt} \quad (12)$$

where, z is a flag equals 0 in heat recovery phase and 1 in adsorption/desorption phase.

Condenser energy balance equation:

$$\left[M_{cond} c_p(T_{cond}) + M_{(HX,Cond)} c_{p,HX}\right] \frac{dT_{cond}}{dt} = h_f \frac{dM_d}{dt} + h_{fg}(T_{cond}) M_a \left(n \cdot \frac{dW_{des}}{dt}\right) + m_{cond} c_p(T_{cond}) \times \left(T_{cond,in} - T_{cond,out}\right) \quad (13)$$

All energy and mass balance equations in addition to adsorbent characteristics equations (isotherms and kinetics) are solved by Simulink with tolerance value of 1×10^{-6}. In this simulation it was assumed that there is no heat loss from the bed and the temperature of all constituents of each component are kept at the same temperature momentarily.

5.2. Validation of numerical model

Results of an experimental test at the operating conditions described in Section 4 and at evaporator and condenser water temperatures of 10 °C were used for validation. Validation of the developed Simulink model is based on a comparison between experimental and numerical temperatures of bed, evaporator and condenser as shown in Fig. 11 showing good agreement between the experimental and simulation results with an error within ±10% which is presented on Table 5. Fig. 12 compares the experimental and numerical results of daily water production and specific cooling power with an error of 7.3 and 6.3% respectively.

The validated mathematical model was used to investigate the system performance at condensing temperature of 30 °C and higher bed heating temperature of 120 °C to achieve the same partial pressure as the case used in the model validation above. Fig. 13 compares the predicted SDWP and SCP to those produced experimentally at condensing

Table 5
Error range for the validation of adsorption desalination cycle.

	Maximum (%)	Minimum (%)
Bed 1	7.59	−8.3
Condenser	0.44	−6.1
Evaporator	5.92	−0.69

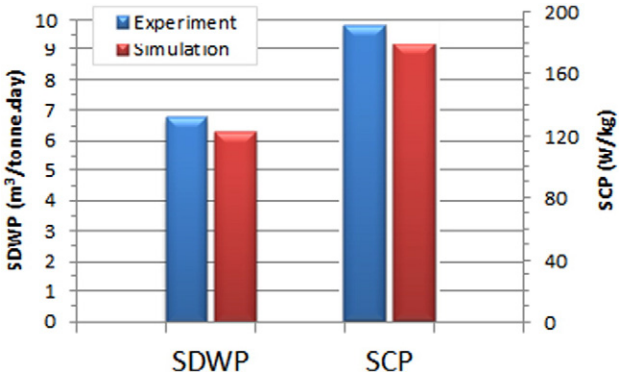

Fig. 12. Comparison of SDWP and SCP for numerical and experimental results for a single-bed adsorption desalination cycle.

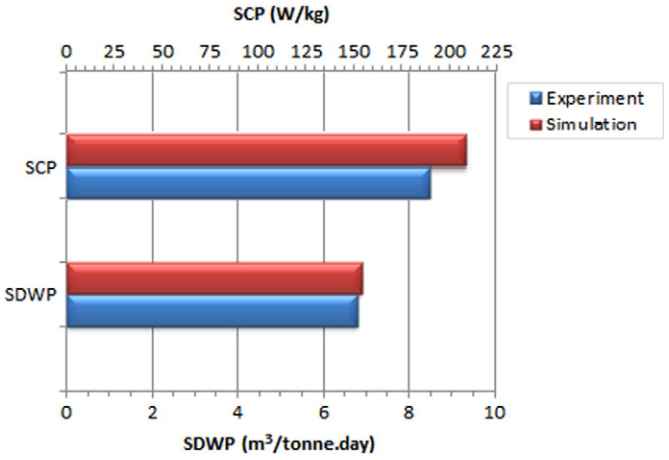

Fig. 13. Comparison of SDWP and SCP for numerical (high desorption and condenser temperatures) and experimental (low desorption and condenser temperatures) results.

temperature of 10 °C and bed heating temperature of 95 °C. It can be seen that they comparable with difference <10%. This illustrates that as long as the partial pressure ratio is maintained, the performance of the system will be comparable.

5.3. Condenser and desorption water temperature effect

SDWP and SCP are shown on Figs. 14 and 15 respectively at further heating medium inlet temperatures for the range of 110–155 °C at

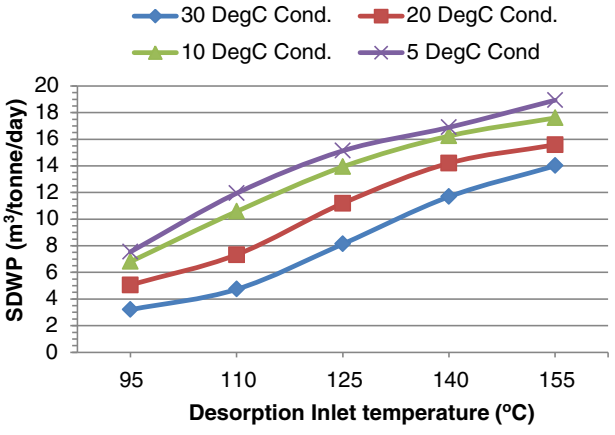

Fig. 14. SDWP at different desorption and condenser water inlet temperatures.

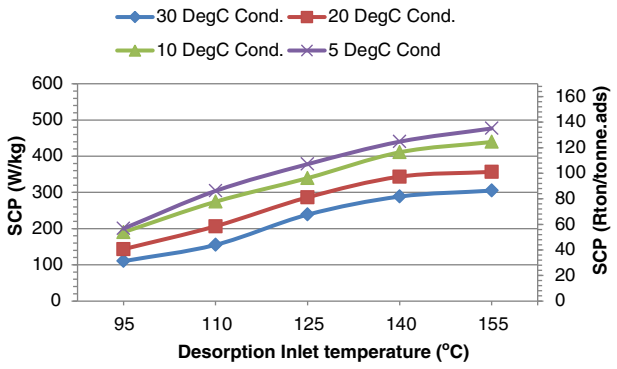

Fig. 15. SCP at different desorption and condenser water inlet temperatures.

different condenser inlet water temperatures ranging from 5 to 30 °C. As noticed from experimental results in Section 4.3, decreasing condenser water inlet temperature results in more cooling and water production where SDWP and SCP increase by 152% and 95% respectively when condenser water inlet temperature decreases from 30 to 5 °C at 110 °C desorption temperature. However, increasing desorption temperature enhances cycle outputs as SDWP and SCP are increased by 195% and 96% when desorption temperature increases from 110 to 155 °C at the same condenser temperature of 30 °C.

6. Conclusions

Adsorption water desalination outperforms conventional desalination technologies in terms of energy consumption, CO_2 emissions and water production cost. MOF is a new class of porous materials with exceptionally high water adsorption capabilities. CPO-27Ni is a MOF material with higher water uptake value at low partial pressure ratio compared to silica gel leading to advantages in terms of water desalination and cooling production. This work experimentally investigates the use of CPO-27Ni MOF adsorbent material for adsorption desalination/cooling applications. The effect of operating parameters like evaporator and condenser water inlet temperatures, half cycle and switching times on the system performance in terms of specific daily water production and specific cooling power were investigated. It was shown that a maximum water production of 22.8 m^3/tonne·ads/day was achieved as well as cooling of 215.9 Rton/tonne adsorbent at maximum evaporator water inlet temperature of 40 °C and condenser water inlet temperature of 5 °C. This is due to the nature of the isotherm curve of CPO-27Ni and the fact that reducing condenser temperature and increasing evaporator temperature, maximizes the cycle uptake and hence results in more cooling and water outputs. In addition, a numerical model was developed and validated using the experimental results and then used to predict cycle performance at other operating conditions. From this model, it was concluded that as long as the partial pressure ratio is maintained, the same cycle outputs could be obtained using different combinations between condenser and desorption temperatures.

Acknowledgement

The authors would like to thank Weatherite Holdings Ltd. for sponsoring the project.

References

[1] H. Ettouney, Seawater desalination, Conventional and Renewable Energ Processes, Springer, 2009.
[2] P.G. Youssef, R.K. Al-Dadah, S.M. Mahmoud, Comparative analysis of desalination technologies, Energy Procedia 61 (2014) 2604–2607.
[3] T. Mezher, H. Fath, Z. Abbas, A. Khaled, Techno-economic assessment and environmental impacts of desalination technologies, Desalination 266 (2011) 263–273.
[4] K. Thu, Adsorption Desalination Theory and Experiment: National University of Singapore, 2010.
[5] J.W. Wu, E.J. Hu, M.J. Biggs, Thermodynamic cycles of adsorption desalination system, Appl. Energy 90 (2012) 316–322.
[6] K.C. Ng, K. Thu, B.B. Saha, A. Chakraborty, Study on a waste heat-driven adsorption cooling cum desalination cycle, Int. J. Refrig. 35 (2012) 685–693.
[7] A. Chakraborty, K. Thu, K.C. Ng, Advanced Adsorption Cooling Cum Desalination Cycle - A Thermodynamic Framework, ASME 2011 International Mechanical Engineering Congress & Exposition IMECE2011, Denver, Colorado, USA, 2011.
[8] K.C. Ng, K. Thu, A. Chakraborty, B.B. Saha, W.G. Chun, Solar-assisted dual-effect adsorption cycle for the production of cooling effect and potable water, International Journal of Low-Carbon Technologies. 4 (2009) 61–67.
[9] J.W. Wu, M.J. Biggs, E.J. Hu, Thermodynamic analysis of an adsorption-based desalination cycle, Chem. Eng. Res. Des. 88 (2010) 1541–1547.
[10] T.X. Li, R.Z. Wang, H. Li, Progress in the development of solid–gas sorption refrigeration thermodynamic cycle driven by low-grade thermal energy, Prog. Energy Combust. Sci. 40 (2014) 1–58.
[11] X. Wang, K.C. Ng, Experimental investigation of an adsorption desalination plant using low-temperature waste heat, Appl. Therm. Eng. 25 (2005) 2780–2789.
[12] K.C. Ng, X.-L. Wang, L. Gao, A. Chakraborty, B.B. Saha, S. Koyama, A. Akisawa, T. Kashiwagi, Apparatus and Method for Desalination, 2010.
[13] K. Thu, K.C. Ng, B.B. Saha, A. Chakraborty, S. Koyama, Operational strategy of adsorption desalination systems, Int. J. Heat Mass Transf. 52 (2009) 1811–1816.
[14] S. Mitra, P. Kumar, K. Srinivasan, P. Dutta, Performance evaluation of a two-stage silica gel + water adsorption based cooling-cum-desalination system, Int. J. Refrig. (2015).
[15] P.G. Youssef, S.M. Mahmoud, R.K. Al-Dadah, Effect of evaporator temperature on the performance of water desalination / refrigeration adsorption system using AQSOA-ZO2, International Journal of Environment, Chemical, Ecological, Geological Engineering. 9 (2015) 679–683.
[16] P.G. Youssef, S.M. Mahmoud, R.K. Al-Dadah, Numerical simulation of combined adsorption desalination and cooling cycles with integrated evaporator/condenser, Desalination 392 (2016) 14–24.
[17] S.M. Ali, A. Chakraborty, Adsorption assisted double stage cooling and desalination employing silica gel + water and AQSOA-Z02 + water systems, Energy Convers. Manag. 117 (2016) 193–205.
[18] E. Elsayed, R. Al-Dadah, S. Mahmoud, A. Elsayed, P.A. Anderson, Aluminium fumarate and CPO-27(Ni) MOFs: characterization and thermodynamic analysis for adsorption heat pump applications, Appl. Therm. Eng. 99 (2016) 802–812.
[19] A. Elsayed, R. AL-Dadah, S. Mahmoud, B. Shi, P. Youssef, A. Elshaer, W. Kaialy, Characterisation of CPO-27Ni Metal Organic Framework Material for Water Adsorption, SUSTEM International ConferenceNewcastle Upon Tyne 2015, pp. 284–290.
[20] A. Elsayed, E. Elsayed, R. Al-Dadah, S. Mahmoud, A. Elshaer, W. Kaialy, Thermal energy storage using metal–organic framework materials, Appl. Energy (2016).
[21] E. Elsayed, R. Al-Dadah, S. Mahmoud, P.A. Anderson, A. Elsayed, P.G. Youssef, CPO-27(Ni), aluminium fumarate and MIL-101(Cr) MOF materials for adsorption water desalination, Desalination (2016), http://dx.doi.org/10.1016/j.desal.2016.07.030.
[22] S.K. Henninger, M. Schicktanz, P.P.C. Hügenell, H. Sievers, H.M. Henning, Evaluation of methanol adsorption on activated carbons for thermally driven chillers part I: thermophysical characterisation, Int. J. Refrig. 35 (2012) 543–553.
[23] B. Shi, R. Al-Dadah, S. Mahmoud, A. Elsayed, E. Elsayed, CPO-27(Ni) metal–organic framework based adsorption system for automotive air conditioning, Appl. Therm. Eng. 106 (2016) 325–333.
[24] L.X. Gong, R.Z. Wang, Z.Z. Xia, C.J. Chen, Design and performance prediction of a new generation adsorption chiller using composite adsorbent, Energy Convers. Manag. 52 (2011) 2345–2350.
[25] J.W. Wu, M.J. Biggs, P. Pendleton, A. Badalyan, E.J. Hu, Experimental implementation and validation of thermodynamic cycles of adsorption-based desalination, Appl. Energy 98 (2012) 190–197.
[26] K.C. Ng, K. Thu, Y. Kim, A. Chakraborty, G. Amy, Adsorption desalination: an emerging low-cost thermal desalination method, Desalination 308 (2013) 161–179.